AGU ADVANCING EARTH AND SPACE SCIENCES

Geophysical Research Letters®

Key Points:

- A high-resolution broadband Lg-wave attenuation model is constructed for Colombia and the surrounding areas
- Lg waves attenuate strongly in the hot active crust above oceanic plate subduction zones and weakly in the cold stable Guiana Shield crust
- A triple junction among the Caribbean, Nazca, and South American Plates is located at approximately 7.5°N, 77°W, as speculated by abrupt variations of seismic attenuation and velocity

Correspondence to:

L.-F. Zhao,
zhaolf@mail.iggcas.ac.cn

Author Contributions:

Conceptualization: Zhen Liu, Lian-Feng Zhao, Carlos A. Vargas
Data curation: Zhen Liu, Lian-Feng Zhao, Bao-Feng Tian
Formal analysis: Zhen Liu, Lian-Feng Zhao
Funding acquisition: Lian-Feng Zhao, Zhen-Xing Yao
Investigation: Zhen Liu, Lian-Feng Zhao
Methodology: Lian-Feng Zhao, Xiao-Bi Xie
Project administration: Lian-Feng Zhao, Zhen-Xing Yao
Resources: Lian-Feng Zhao
Software: Zhen Liu, Lian-Feng Zhao, Xiao-Bi Xie, Zhen-Xing Yao

A New High-Resolution Broadband Lg Attenuation Model Beneath Colombia: Implications for Triple Junction Tectonics

Zhen Liu[1,2], **Lian-Feng Zhao**[1,3] , **Xiao-Bi Xie**[4], **Carlos A. Vargas**[5] , **Bao-Feng Tian**[6], and **Zhen-Xing Yao**[1]

[1]Key Laboratory of Planetary Science and Frontier Technology, Institute of Geology and Geophysics, Chinese Academy of Sciences, Beijing, China, [2]College of Earth and Planetary Sciences, University of Chinese Academy of Sciences, Beijing, China, [3]Heilongjiang Mohe Observatory of Geophysics, Institute of Geology and Geophysics, Chinese Academy of Sciences, Beijing, China, [4]Institute of Geophysics and Planetary Physics, University of California at Santa Cruz, Santa Cruz, CA, USA, [5]Department of Geosciences, Universidad Nacional de Colombia, Bogotá, Colombia, [6]Institute of Geophysics, China Earthquake Administration, Beijing, China

Abstract The existence of a typical triple junction in Colombia is crucial for understanding plate convergence and coupling among the South American Plate, the subducting Nazca Plate, and the Caribbean Plate. However, locating this triple junction is challenging due to complex geodynamic evolution and uncertainty in the slab boundaries. Here, we developed a high-resolution Lg-wave attenuation model for Colombia and surrounding areas to constrain crustal magmatic activity, link deep processes with surface volcanism, and identify potential slab boundaries. The area encompassing Central America, western Colombia, and Ecuador exhibits strong Lg attenuation and a concentration of volcanoes, indicating thermal anomalies in the crust. In line with velocity structure, volcanism, seismicity, and isotopic dating, the thermal anomalies caused by the subducting Nazca and Caribbean slabs suggest the presence of three subducting slabs beneath the South American Plate, with a triple junction located at approximately 7.5°N, 77°W.

Plain Language Summary The complex tectonics of Colombia and its surrounding regions result from the convergence of three tectonic plates, the South American, Caribbean, and Nazca plates. Their convergence forms a "triple junction," but it sank beneath the South American due to plate interaction, and its exact location remains uncertain. Seismic Lg waves that travel through Earth's crust can be used to measure crustal attenuation via their amplitude decay, providing constraints on the thermal structure of the Colombian crust. In this study, we constructed a high-resolution broadband Lg attenuation model for Colombia and the surrounding areas. The cold, stable Guiana Shield is characterized by weak Lg attenuation. In contrast, the active volcanic regions in Central America and western Colombia exhibit strong Lg attenuation. Abrupt changes in attenuation patterns suggest that the slabs subducting north and south of 7.5°N belong to the Caribbean and Nazca plates, respectively. Thus, the point at 7.5°N, 77°W may be the sunken triple junction among the South American, Caribbean, and Nazca plates.

1. Introduction

McKenzie and Morgan (1969) proposed that a triple junction is the point where three plate boundaries intersect and that various types of triple junctions occur worldwide. At a triple junction, the interactions among the three plates reflect the history of their mutual movements. Therefore, the current location of a triple junction can serve as a boundary condition for tectonic evolution and hence plays a vital role in investigating plate collisions. In Colombia and adjacent regions, the South American Plate, the Nazca Plate, and the Caribbean Plate meet at a TTF (Trench, Trench, and Transform Fault)-type triple junction, located in the Panama-Choco Arc (PCA) (González et al., 2023; Kellogg et al., 2019; Wang & Wei, 2018). The complex tectonic setting of this triple junction was shaped by the subduction and collision of multiple plates (Figure 1) (Hey, 1977; Kellogg et al., 1995; Pennington, 1981; Taboada et al., 2000). These processes have generated complex features, including the Cordillera uplift in northwestern Colombia and widespread trenches, deformation zones, fault systems, and back-arc volcanoes. The eastern part of the South American Plate at these latitudes is dominated by the Guiana Shield, which formed during the Precambrian (Schmitz et al., 2002). Plate interactions in Colombia result in intense seismic activity, producing two zones of concentrated intermediate-depth earthquakes: the Bucaramanga and Cauca Nests

Supervision: Lian-Feng Zhao, Xiao-Bi Xie, Zhen-Xing Yao
Validation: Zhen Liu, Lian-Feng Zhao
Visualization: Zhen Liu, Bao-Feng Tian
Writing – original draft: Zhen Liu
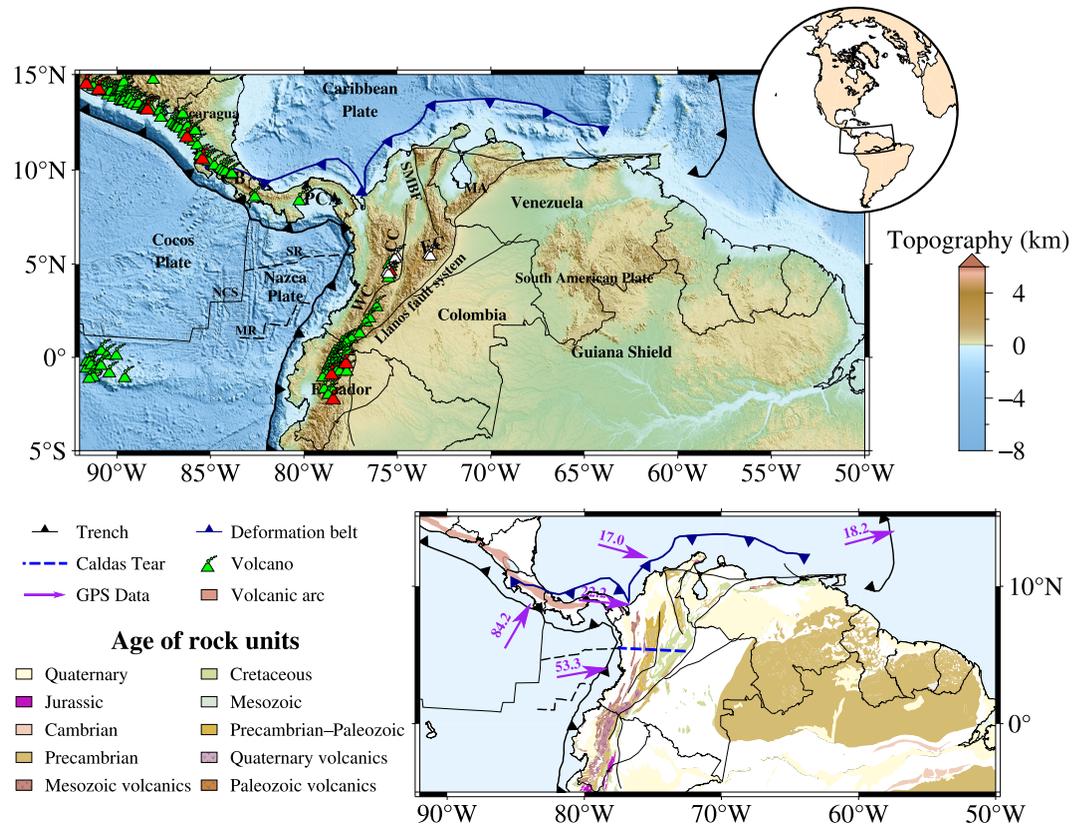**Writing – review & editing:** Zhen Liu, Lian-Feng Zhao, Xiao-Bi Xie, Carlos A. Vargas, Bao-Feng Tian

Figure 1. Map showing the main tectonics and simplified geologic setting in and around Colombia. Overlaid on the map are major faults (Veloza et al., 2012); geologic provinces (Schenk et al., 1999); the GPS-derived movement velocity vectors (mm/yr) (purple arrows) of the Nazca, Cocos, and Caribbean Plates relative to the stable South American Plate (Jarrin et al., 2023; Mora-Páez et al., 2019); and surface volcanoes, including dormant volcanoes (white triangles), active volcanoes (green triangles), and volcanoes with eruption records in 2023 (red triangles) (Global Volcanism Program, 2023). The blue dashed line marks the Caldas Tear (C. A. Vargas & Mann, 2013). The abbreviations are as follows: WC, Western Cordillera; CC, Central Cordillera; EC, Eastern Cordillera; SMBF, Santa Marta-Bucaramanga Fault; MA, Merida Andes; PCA, Panama-Choco Arc; CB, Chorotega Block; NCS, Nazca-Cocos Spreading Center; SR, Sandra Ridge; MR, Malpelo Ridge.

(Figure S1a in Supporting Information S1) (Pérez-Forero et al., 2023). The two seismic nests are longitudinally offset at approximately 5.5°N, which may indicate the tearing of the underlying subducting slab, known as the Caldas Tear (Idárraga-García et al., 2016; C. A. Vargas & Mann, 2013). The location of the triple junction can move along the slab boundary between the subducting Nazca and Caribbean slabs beneath Northwest South America (NWSA) (Boschman et al., 2014; González et al., 2023; Montes et al., 2019). However, the location of the boundary between the subducting Nazca and Caribbean slabs has long been controversial.

Multiple models have been suggested for the boundary between the Nazca and Caribbean slabs (e.g., Pennington, 1981; Sun et al., 2022; Syracuse et al., 2016; C. A. Vargas & Mann, 2013). Historical seismicity reveals that a shear zone near 5.2°N is likely the boundary between the Nazca and Caribbean slabs (Pennington, 1981). The receiver function and velocity tomography results suggest that the Nazca and Caribbean slabs partially overlap without a clear boundary (Boada et al., 2022; Sun et al., 2022; Taboada et al., 2000). Gravitational, magnetic, and Coda Q images reveal that the collision between the PCA and NWSA produced V-shaped crustal deformation, which may have triggered the Nazca slab tear along 5.5°N (C. A. Vargas & Mann, 2013). The Nazca slab is tearingly split into the Cauca segment to the south and the Bucaramanga segment to the north, with the boundary between the Nazca and Caribbean slabs located at 7.5°N (Syracuse et al., 2016). On the other hand, the presence of volcanic arcs is closely related to the subduction angle (Coira et al., 1982; Wagner et al., 2017). Typically, in steep subduction zones, deep magma rises to form volcanic arcs, whereas in flat subduction zones, the supply of subsurface magma diminishes, resulting in the absence of surface volcanoes (Gutscher et al., 2000; Ramos et al., 2002). Due to the influence of subducting slabs from different time intervals and angles, the magmatic

activity in the crust of NWSA is diverse and discontinuous, resulting in different rheological properties and thermal structures of individual blocks (Lagardère & Vargas, 2021; Vargas et al., 2015, 2019). Compared to wave speed, seismic attenuation is more sensitive to the temperature and rheological properties of deep materials (Boyd et al., 2004; Zhao, Xie, He, et al., 2013). Therefore, we develop an attenuation model to investigate the crustal thermal structure due to subducting slabs and infer the potential triple junction beneath Colombia.

Seismic Lg waves are a prominent phase in high-frequency regional seismograms (e.g., Gutenberg, 1955; Kennett, 1984; Oliver & Ewing, 1957). These waves can be considered the superposition of higher-order surface waves or multiple supercritical reflected shear waves in crustal waveguides (e.g., Bouchon, 1982; Knopoff et al., 1973; Xie & Lay, 1994). Lg waves carry rich information about crustal structure and composition and have been widely used to investigate attenuation in the crust (Bowman & Kennett, 1991; Mitchell et al., 1997; Ottemöller, 2002; Zhang et al., 2022; Zhao et al., 2010). The thermal structures of the crust and mantle have been altered by extensive tectonic deformation, intense magmatism, and seismic activity resulting from plate subduction and tearing in the region (Cediel and Shaw, 2019). Seismic Lg-wave attenuation can indicate the distribution of crustal thermal anomalies (e.g., Yang et al., 2024). Thus, by combining seismic activity with other geophysical and geological observations, Lg attenuation provides an opportunity to constrain the crustal thermal structure in Colombia and adjacent regions, offering insight into locating the triple junction by identifying the boundary of the subducting slab.

2. Data and Methods

We collected 10,633 vertical-component regional waveforms from 563 earthquakes in Colombia and adjacent regions recorded at 168 broadband digital seismic stations between 2000 and 2023 (Figure S1b in Supporting Information S1, Tables S1 and S2 in Supporting Information S2). Lg waveforms were selected within an epicentral distance range of 200–3000 km (Figure S2 in Supporting Information S1) (Zhao, Xie, Wang, et al., 2013; Zhao et al., 2010). The focal depths of the selected events are shallower than the Moho depth provided by the CRUST1.0 model (Table S1 in Supporting Information S2) (Laske et al., 2013). To ensure good signal-to-noise ratios and avoid the effects of complex rupture processes resulting from large earthquakes, we selected events with magnitudes between 4.0 and 6.0. Only stations that recorded three or more events and events recorded at three or more stations were used.

We sampled the Lg wave signal using a 3.0–3.6 km/s group velocity window and extracted the pre-P and pre-Lg noise sequences with the same length as the Lg wave signal sampling window (e.g., Ma et al., 2023; Zhao et al., 2010). Then, the amplitude spectra of the Lg wave, pre-P noise, and pre-Lg noise were calculated using the Fast Fourier Transform algorithm. A high-quality Lg-wave spectral data set was obtained after noise correction (Figure S3 in Supporting Information S1) (e.g., Luo et al., 2021). Next, we established a joint inversion system for the Q_{Lg} value, source term, and site response using amplitude spectra and spectral ratios (Zhao et al., 2010, 2022). A linear inversion system was solved using the least squares QR factorization algorithm with damping and smoothing, which converted the observed Lg amplitudes to Q_{Lg} values (e.g., Paige & Saunders, 1982; Phillips & Stead, 2008). Finally, a broadband Q_{Lg} model was obtained via independent inversion at each frequency.

After the inversion, the data residuals tended to follow a Gaussian distribution with a zero mean and a minimum standard deviation (Figure S4 in Supporting Information S1). To verify the robustness of the results and system stability, we analyzed the spatial resolution of Lg-wave tomography using the checkerboard method (e.g., He et al., 2021; Zhao, Xie, He, et al., 2013) and assessed the standard errors using the bootstrap technique (Efron, 1983). The tomographic resolution can reach $1° \times 1°$ or higher, indicating the reliability of our results (Figure 2d). The mean Q_{Lg} map (Figure S5a in Supporting Information S1) agrees well with the directly inverted result (Figure 2e), and the standard deviation is much smaller than the mean Q_{Lg}, ranging from 0 to 40 (Figure S5b in Supporting Information S1). Therefore, the inversion system and amplitude data can provide a stable estimate of crustal attenuation for this region. Recently, the above-mentioned Lg-wave attenuation tomography method has been successfully applied worldwide (e.g., He et al., 2021; Shen et al., 2023; Yang et al., 2023; Zhao, Xie, He, et al., 2013; Zhu et al., 2023).

3. Results

The attenuation model for Colombia and its adjacent areas comprises Q_{Lg} distributions at 58 individual frequencies, ranging from 0.05 to 10.0 Hz (e.g., Figures 2a and 2b). However, the Q_{Lg} between 0.2 and 2.0 Hz can
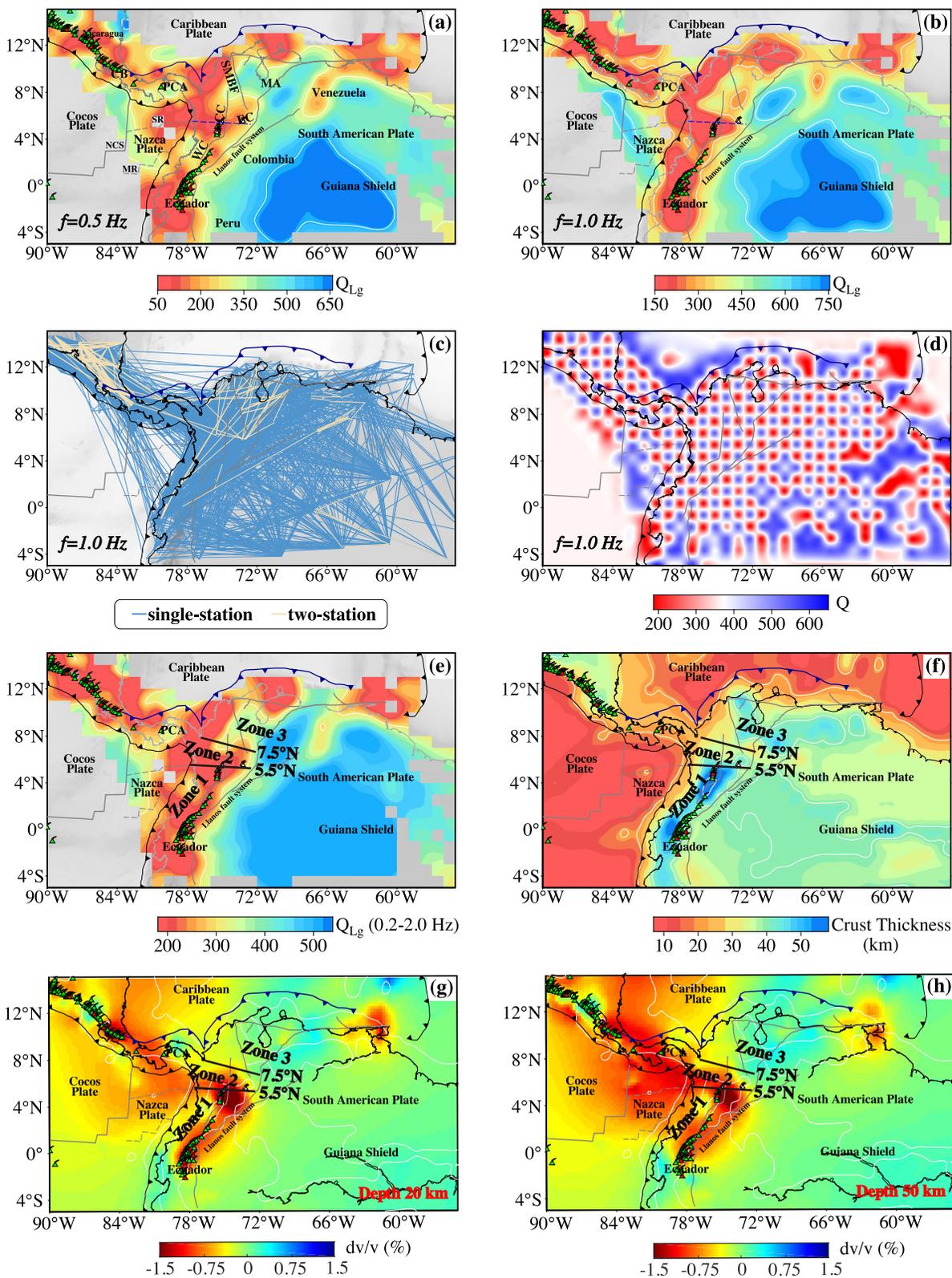
Figure 2.

better characterize the geological blocks compared with other frequency bands (Figure S6 in Supporting Information S1). The Q_{Lg} values increase with increasing frequency, and the lateral variations of Q_{Lg} correspond well with the regional tectonics and the P-wave velocities (Figure 2). The nonlinear relationship between Q_{Lg} values and crustal thickness indirectly indicates that geological blocks undergoing strong attenuation may be more strongly influenced by factors such as temperature or fluid content (Figure 2f and Table S3 in Supporting Information S2).

The Guiana Shield comprises the Proterozoic and Paleozoic terranes, forming a stable continental craton with a thick crust, high-velocity lithospheric anomalies, and weak attenuation anomalies (Figures 2e–2h; Bezada et al., 2010; Mendoza, 1977; Schmitz et al., 2002). High-Q_{Lg} anomalies in western Venezuela correlate with previously observed high-velocity features, potentially linked to ancient Caribbean slab subduction (Lü et al., 2022; Miller et al., 2009; van Benthem et al., 2013). The Central American Volcanic Arc, along with volcanic zones in western Colombia and Ecuador, shows low-Q_{Lg} features consistent with known Lg-wave attenuation and low-velocity structures, suggesting widespread high-temperature anomalies or partial melting in the crust (Lü et al., 2022; Ojeda & Ottemöller, 2002; Syracuse et al., 2008; Zhu et al., 2020). The Caldas Tear at 5.5°N is substantiated by various findings, including the cessation of volcanic activity to the north (Wagner et al., 2017), a shift in seismic activity (C. A. Vargas & Mann, 2013), and analyses of adakitic samples from the Nevado del Ruiz volcano (Borrero et al., 2009; Garcia et al., 2019). Therefore, we propose that underground hydrothermal upwelling channels are induced by slab tearing based on the extensive and pronounced low-Q_{Lg} features in this region.

4. Discussion

The Nazca-Caribbean-South America (NCS) triple junction has been migrating continuously northward along the trench west of Colombia (Figure 4a) (González et al., 2023). The PCA formed between the Nazca and Caribbean Plates in the Cretaceous, and as the Caribbean Plate migrated eastward during the Paleocene, the PCA gradually approached the NWSA (Buchs et al., 2010; Pindell et al., 2006). Until approximately 15 Ma, the PCA collided with the NWSA, causing this triple junction to vanish from the surface and become buried beneath the NWSA (Boschman et al., 2014; Farris et al., 2011). Consequently, the juncture where the subducting Nazca slab interfaces with the Caribbean slab became the current location of the NCS triple junction. However, divergent convergent boundaries were obtained between the Nazca and Caribbean slabs using different geophysical methods, such as those from seismic velocity tomography, receiver function imaging, and seismicity analysis (Boada et al., 2022; Sun et al., 2022; E. M. Syracuse et al., 2016; Taboada et al., 2000). Thus, the subduction processes and the location of the triple junction remain debated. Slab subduction can induce mantle upwelling, significantly affecting the crust's thermal structure. On the other hand, strong Lg-wave attenuation can indicate the distribution of crustal thermal anomalies (e.g., Yang et al., 2024). Therefore, the lateral variation in seismic Lg-wave attenuation is an indicator of the convergent boundaries of subducting slabs at the crustal scale, which can constrain the current location of the triple junction and reveal the deep dynamical mechanism underlying the disappearance of the triple junction at the surface.

The collision of the PCA with NWSA induces tearing of the Nazca slab along the Sandra Ridge at approximately 5.5°N (C. A. Vargas & Mann, 2013). The Nazca slab can be divided into two segments: the Bucaramanga segment in the north and the Cauca segment in the south (Syracuse et al., 2016). Therefore, the subduction zone in NWSA comprises three distinct slabs (Zones 1–3 in Figure 2e), corresponding to the Caribbean slab and Bucaramanga and Cauca segments from the Nazca slab. The Cauca segment subducts at a relatively steep angle (∼30°–40°) (C. A. Vargas & Mann, 2013). The slab dehydration induces mantle melting, causing hot material to upwell and form crustal magma chambers and surface volcanic arcs (Zone 1 in Figure 2e) (Sun et al., 2022; C. A. Vargas & Mann, 2013; Wagner et al., 2017). Consequently, a low-Q_{Lg} anomaly is observed in Zone 1, with Q_{Lg} values ranging from 50 to 160 at 1 Hz (Figures 2e and 3a), which is consistent with previous findings of a 1 Hz

Figure 2. Comparison among crustal Lg-wave attenuation model, crustal thickness, and velocity model for Colombia and surrounding areas. (a, b) Selected crustal Q_{Lg} maps at 0.5 and 1.0 Hz. (c, d) Ray coverage and resolution analyses at 1.0 Hz. Both two-station (light yellow) and single-station (blue) ray paths are presented. The checkerboard resolution tests were conducted at 1° × 1°. (e) 0.2–2.0 Hz broadband Q_{Lg} distribution. (f) Crustal thickness extracted from the CRUST1.0 model (Laske et al., 2013). (g, h) Lateral variations in P-wave velocity perturbation according to the MITP_USA_2016MAY model at depths of 20 and 50 km (Burdick et al., 2017). Note that in the Q_{Lg} maps, some Q_{Lg} distributions are excluded due to weak ray coverage. The colored triangle symbols represent volcanoes, as illustrated in Figure 1.
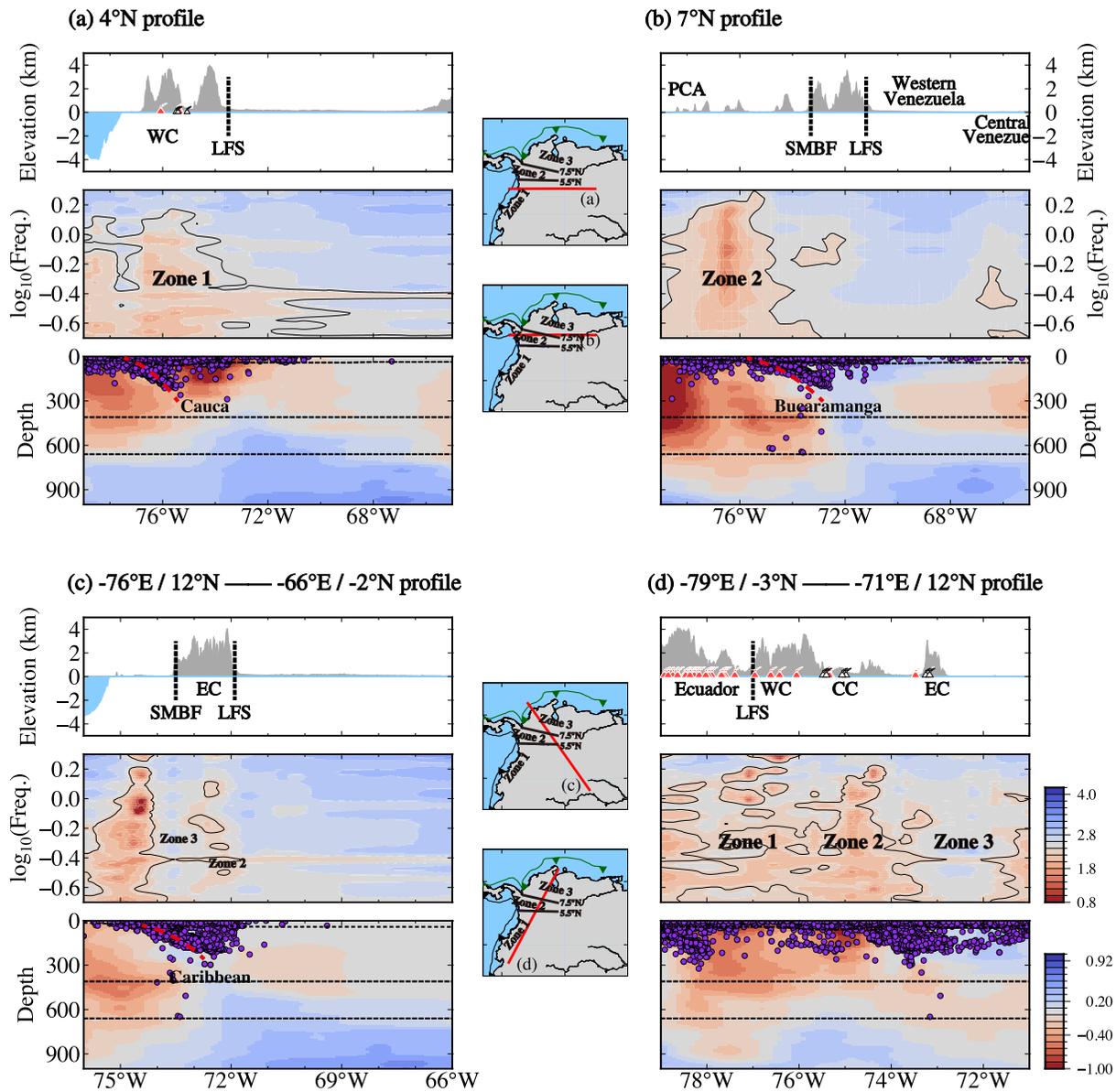
Figure 3. Comparison of various geological and geophysical data along four cross-sections (a–d). The locations of the profiles are indicated in the inset maps using red lines. Each profile is composed of three panels. The top panel shows the surface topography and locations of major faults (vertical dashed lines). The middle panel shows Q_{Lg} as a function of frequency. The bottom panel shows the P-wave velocity perturbations (Burdick et al., 2017) and regional seismicity above magnitude two between 1900 and 2023 (purple circles) from the IRIS. The black dashed lines indicate the Moho discontinuity and the 410-km and 660-km mantle interfaces. The Moho depth is extracted from CRUST 1.0 (Laske et al., 2013). LFS refers to the Llanos Fault System. The other abbreviations for geological blocks and major faults are the same as those in Figure 1.

Q_{Lg} value of ∼150 (Ojeda & Ottemöller, 2002). Zone 1 is characterized by low velocities with a 1.5% low-velocity perturbation at 20 and 50 km (Figures 2g and 2h) (Burdick et al., 2017), as well as a low-velocity perturbation of up to 0.25 km/s for Pn waves propagating through the uppermost mantle (Lü et al., 2022). In contrast, the Bucaramanga segment subducts at a low angle (Zone 2 in Figure 2e), characterized by relatively strong Lg attenuation, low S-wave velocities, high Vp/Vs ratios, and the absence of active surface volcanism (Figures 2e and 3b) (Bernet et al., 2016; Boada et al., 2022; Monsalve et al., 2019; Ojeda & Ottemöller, 2002; Pardo et al., 2005; Poveda et al., 2018). Before the development of the Caldas Tear at approximately 4 Ma, surface volcanism in Zones 1 and 2 had a similar pattern, reaffirming that both the Cauca and Bucaramanga segments originated from the Nazca slab (Figure S7 in Supporting Information S1) (Wagner et al., 2017). Around 12 Ma, subduction of the Nazca slab and collision between the PCA and the NWSA led to thickening of the oceanic crust
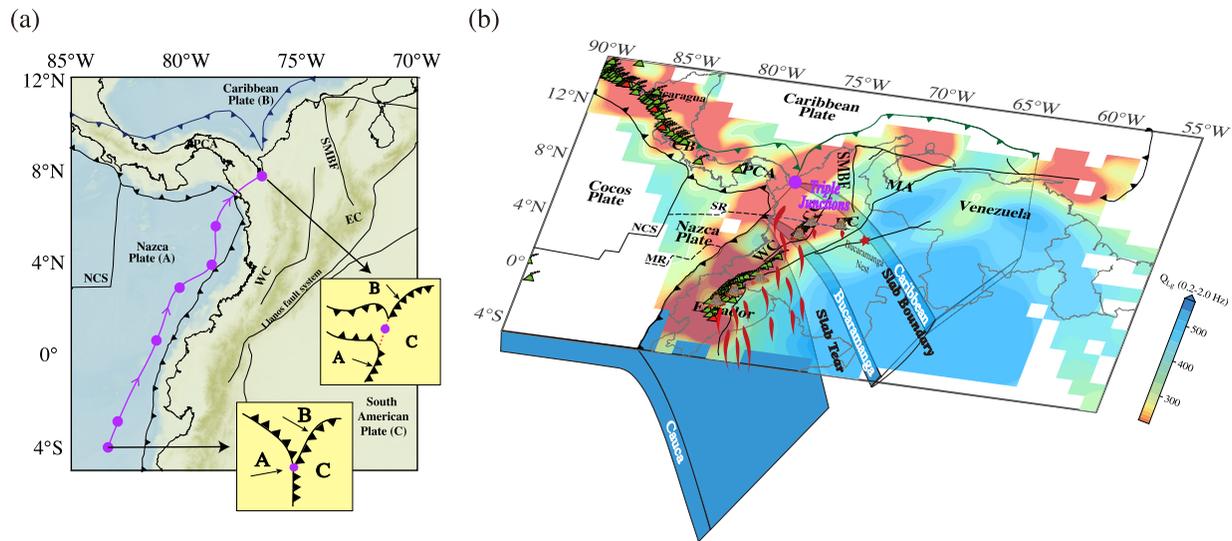
Figure 4. (a) The migration of the NCS triple junction (purple circles) with geological ages (González et al., 2023). Initially, this triple junction was marked on the surface, but it later disappeared due to the collision between the PCA and NWSA. The intersection of the Nazca and Caribbean slabs in the lithosphere beneath the South American Plate may be the location of the present triple junction. (b) Diagram showing the proposed tectonic activities of the Nazca and Caribbean slabs beneath NWSA. The observed broadband Q_{Lg} data between 0.2 and 2.0 Hz are projected on the top surface. The different angles of subduction of the northern and southern slabs due to the tearing of the Nazca slab, as well as the subducting Caribbean slab, are observed, as indicated by previous velocity tomography (Figures S8 and S9 in Supporting Information S1) (Li et al., 2008). Slab subduction and tearing are the primary factors driving the upwelling of hot material (red streaks), which leads to the formation of surface volcanism. Based on surface volcanism and sharp changes in attenuation to the north and south of 7.5°N, as well as the velocity tomography and receiver function results (Figures S8 and S9 in Supporting Information S1) (Boada et al., 2022; Syracuse et al., 2016), we speculate that 7.5°N marks the boundary separating the Nazca and Caribbean slabs. The proposed triple junction, marked in a purple circle, is primarily based on tectonic activity and substantial changes in Lg attenuation.

beneath Zone 2, with high buoyancy, which sustained flat subduction (Lonsdale, 2005). Additionally, the velocity images and seismic activities indicate the presence of two subducting slabs, with steep and flat subduction zones underneath Zones 1 and 2, respectively (Figures 3a and 3b) (Burdick et al., 2017). Therefore, there is no active volcanism in Zone 2, and the low-Q_{Lg} signature beneath it is likely due to thermal upwelling from Nazca slab tearing and residual heat from the dormant volcanic crust.

The Caribbean-Nazca slab boundary is likely at approximately 7.5°N, which features significant Q_{Lg} variations (Figure 2e). Zone 3 exhibits high crustal Q_{Lg} values and high upper-mantle velocities compared to Zones 1 and 2, suggesting the presence of a subducting Paleo-Caribbean slab beneath Zone 3 (Figures 2 and 3) (Lü et al., 2022). The Caribbean Plate, which formed during the Late Cretaceous, is a thick, buoyant oceanic plateau (Burke, 1988; Pindell et al., 2006). Paleomagnetic analysis results indicate that the Caribbean slab subducted flatly beneath the NWSA from the Middle Eocene to the present (Müller et al., 2019; Seton et al., 2012). The Caribbean large igneous province, which formed since the Cretaceous, increased the oceanic crustal thickness, allowing it to resist slab hydration at flexures, normal faults, and trenches, and preventing partial melting of the mantle wedge (Syracuse et al., 2010). Thus, volcanism ceased when the flat subduction of the Caribbean slab initiated (Syracuse et al., 2016), resulting in weak-attenuation characteristics in the crust of Zone 3 (Figures 2 and 3). $^{40}Ar/^{39}Ar$ isotopic dating revealed a magmatic intrusion with an age of approximately 15–7 Ma in Zone 2, which originates from dehydration melting of the subducting Nazca slab (Leal-Mejía et al., 2019; Wagner et al., 2017; Weber et al., 2020). If the Caribbean slab exists in Zone 2, these magmatic activities can be blocked from rising to the surface; therefore, this indirectly suggests the Caribbean slab has not intruded into Zone 2 since the Late Miocene (González et al., 2023). Consequently, the Caribbean slab is confined north of 7.5°N. The boundary between the Nazca and Caribbean slabs extends from the subducted slab conjunction at the northern end to the Bucaramanga seismic nest at the southern end. Therefore, by integrating crustal Q_{Lg} values, seismic velocity tomography, and seismicity distribution, we obtain a triple junction tectonic model of the three subducting slabs beneath the NWSA (Figure 4b). The current location of the NCS triple junction is approximately 7.5°N, 77°W (Figure 4b).

5. Conclusion

We developed a broadband Lg-wave attenuation model for Colombia and its surroundings with a spatial resolution of $1° \times 1°$ using a joint inversion method based on single- and two-station data. The lateral variation in the Q_{Lg} values appears to be correlated with tectonics. The Guiana Shield is an ancient, cold, and stable craton characterized by high Q_{Lg} and weak attenuation properties. In contrast, active, hot, and unstable volcanic areas, including Central America, western Colombia, and Ecuador, exhibit low QLg values and strong attenuation, associated with the upwelling of hot material resulting from dehydration during plate subduction and partial melting of the mantle wedge. Combining our model with previous studies, including velocity imaging, receiver function analysis, tectonic reconstruction, etc., we found that the collision of the PCA with NWSA caused the Nazca slab to tear at 5.5°N, exhibiting strong attenuation features (Boada et al., 2022; González et al., 2023; Syracuse et al., 2016). South of the tear is the steeply subducting Cauca segment, characterized by strong attenuation, whereas to the north is the relatively strong attenuation, flatly subducting Bucaramanga segment. The weakly attenuating feature north of 7.5°N likely indicates an earlier subducting Paleo-Caribbean slab beneath South America. Thus, three subducting slabs exist beneath NWSA, and approximately 7.5°N, 77°W may be considered the current location of the NCS triple junction within the Colombian tectonic regime (Figure 4b).

Conflict of Interest

The authors declare no conflicts of interest relevant to this study.

Data Availability Statement

Waveform and station metadata were downloaded using Obspy (Krischer et al., 2015) through the International Federation of Digital Seismograph Networks webservices and obtained from several data-sharing centers, such as the Incorporated Research Institutions for Seismology Data Management Center and the GEOFON Data Management Center; the corresponding website links are listed in Tables S2 and S4 in Supporting Information S2. The single- and two-station Lg amplitude data used in this study, along with the resulting Lg-wave attenuation model for Colombia and its vicinity, are available in Liu et al. (2024). Specific figures were generated using Generic Mapping Tools (Wessel et al., 2019).

References

Bernet, M., Urueña, C., Amaya, S., & Peña, M. L. (2016). New thermo and geochronological constraints on the Pliocene-Pleistocene eruption history of the Paipa-Iza volcanic complex, Eastern Cordillera, Colombia. *Journal of Volcanology and Geothermal Research*, *327*, 299–309. https://doi.org/10.1016/j.jvolgeores.2016.08.013

Bezada, M. J., Levander, A., & Schmandt, B. (2010). Subduction in the southern Caribbean: Images from finite-frequency P wave tomography. *Journal of Geophysical Research*, *115*(B12), 2010JB007682. https://doi.org/10.1029/2010JB007682

Boada, M. J. M., Poveda, E., & Tary, J. B. (2022). Lithospheric and slab configurations from receiver function imaging in northwestern South America, Colombia. *Journal of Geophysical Research-Solid Earth*, *127*(12), e2022JB024475. https://doi.org/10.1029/2022JB024475

Borrero, C., Toro, L. M., Alvarán, M., & Castillo, H. (2009). Geochemistry and tectonic controls of the effusive activity related with the ancestral Nevado del Ruiz volcano, Colombia. *Geofísica Internacional*, *48*(1). https://doi.org/10.22201/igeof.00167169p.2009.48.1.105

Boschman, L. M., van Hinsbergen, D. J. J., Torsvik, T. H., Spakman, W., & Pindell, J. L. (2014). Kinematic reconstruction of the Caribbean region since the early Jurassic. *Earth-Science Reviews*, *138*, 102–136. https://doi.org/10.1016/j.earscirev.2014.08.007

Bouchon, M. (1982). The complete synthesis of seismic crustal phases at regional distances. *Journal of Geophysical Research*, *87*(B3), 1735–1741. https://doi.org/10.1029/JB087iB03p01735

Bowman, J. R., & Kennett, B. L. N. (1991). Propagation of Lg waves in the North Australian Craton: Influence of crustal velocity gradients. *Bulletin of the Seismological Society of America*, *81*(2), 592–610.

Boyd, O. S., Jones, C. H., & Sheehan, A. F. (2004). Foundering lithosphere imaged beneath the Southern Sierra Nevada, California, USA. *Science*, *305*(5684), 660–662. https://doi.org/10.1126/science.1099181

Buchs, D. M., Arculus, R. J., Baumgartner, P. O., Baumgartner-Mora, C., & Ulianov, A. (2010). Late Cretaceous arc development on the SW margin of the Caribbean Plate: Insights from the Golfito, Costa Rica, and Azuero, Panama, complexes. *Geochemistry, Geophysics, Geosystems*, *11*(7), 2009GC002901. https://doi.org/10.1029/2009GC002901

Burdick, S., Vernon, F. L., Martynov, V., Eakins, J., Cox, T., Tytell, J., et al. (2017). Model update May 2016: Upper-mantle heterogeneity beneath North America from travel-time tomography with Global and USArray Data. *Seismological Research Letters*, *88*(2A), 319–325. https://doi.org/10.1785/0220160186

Burke, K. (1988). Tectonic evolution of the Caribbean. *Annual Review of Earth and Planetary Sciences*, *16*(1), 201–230. https://doi.org/10.1146/annurev.ea.16.050188.001221

Cediel, F. & Shaw, R. P. (Eds.) (2019). *Geology and Tectonics of Northwestern South America: The Pacific-Caribbean-Andean Junction*. Springer International Publishing. https://doi.org/10.1007/978-3-319-76132-9

Coira, B., Davidson, J., Mpodozis, C., & Ramos, V. (1982). Tectonic and magmatic evolution of the Andes of northern Argentina and Chile. *Earth-Science Reviews*, *18*(3–4), 303–332. https://doi.org/10.1016/0012-8252(82)90042-3

Efron, B. (1983). Estimating the error rate of a prediction rule: Improvement on cross-validation. *Journal of the American Statistical Association*, *78*(382), 316–331. https://doi.org/10.1080/01621459.1983.10477973

Farris, D. W., Jaramillo, C., Bayona, G., Restrepo-Moreno, S. A., Montes, C., Cardona, A., et al. (2011). Fracturing of the Panamanian Isthmus during initial collision with South America. *Geology*, *39*(11), 1007–1010. https://doi.org/10.1130/G32237.1

Garcia, M. A., Vargas, C. A., & Koulakov, I. Y. (2019). Local Earthquake Tomography of the Nevado del Huila Volcanic Complex (Colombia): Magmatic and tectonic interactions in a volcanic-glacier complex system. *Journal of Geophysical Research-Solid Earth*, *124*(2), 1688–1699. https://doi.org/10.1029/2018jb016324

Global Volcanism Program. (2023). [Database] Volcanoes of the World (v. 5.1.0; 9 Jun 2023). *Distributed by Smithsonian Institution, compiled by Venzke, E.* https://doi.org/10.5479/si.GVP.VOTW5-2023.5.1

González, R., Oncken, O., Faccenna, C., Le Breton, E., Bezada, M., & Mora, A. (2023). Kinematics and convergent tectonics of the northwestern South American plate during the Cenozoic. *Geochemistry, Geophysics, Geosystems*, *24*(7), e2022GC010827. https://doi.org/10.1029/2022GC010827

Gutenberg, B. (1955). Channel waves in the Earth's crust. *Geophysics*, *20*(2), 283–294. https://doi.org/10.1190/1.1438141

Gutscher, M. A., Spakman, W., Bijwaard, H., & Engdahl, E. R. (2000). Geodynamics of flat subduction: Seismicity and tomographic constraints from the Andean margin. *Tectonics*, *19*(5), 814–833. https://doi.org/10.1029/1999tc001152

He, X., Zhao, L., Xie, X., Tian, X., & Yao, Z. (2021). Weak crust in southeast Tibetan Plateau revealed by Lg-Wave attenuation tomography: Implications for crustal material escape. *Journal of Geophysical Research: Solid Earth*, *126*(3), e2020JB020748. https://doi.org/10.1029/2020JB020748

Hey, R. (1977). Tectonic evolution of the Cocos-Nazca spreading center. *Geological Society of America Bulletin*, *88*(10), 1404. https://doi.org/10.1130/0016-7606(1977)88<1404:TEOTCS>2.0.CO;2

Idárraga-García, J., Kendall, J.-M., & Vargas, C. A. (2016). Shear wave anisotropy in northwestern South America and its link to the Caribbean and Nazca subduction geodynamics. *Geochemistry, Geophysics, Geosystems*, *17*(9), 3655–3673. https://doi.org/10.1002/2016GC006323

Jarrin, P., Nocquet, J. M., Rolandone, F., Mora-Paez, H., Mothes, P., & Cisneros, D. (2023). Current motion and deformation of the Nazca Plate: New constraints from GPS measurements. *Geophysical Journal International*, *232*(2), 842–863. https://doi.org/10.1093/gji/ggac353

Kellogg, J. N., Camelio, G. B. F., & Mora-Páez, H. (2019). Cenozoic tectonic evolution of the North Andes with constraints from volcanic ages, seismic reflection, and satellite geodesy. In *Andean Tectonics* (pp. 69–102). Elsevier. https://doi.org/10.1016/B978-0-12-816009-1.00006-X

Kellogg, J. N., Vega, V., Stailings, T. C., & Aiken, C. L. V. (1995). Tectonic development of Panama, Costa Rica, and the Colombian Andes: Constraints from Global Positioning System geodetic studies and gravity. In *Geological Society of America Special Papers* (Vol. 295, pp. 75–90). Geological Society of America. https://doi.org/10.1130/SPE295-p75

Kennett, B. L. N. (1984). Guided wave propagation in laterally varying media—I. Theoretical development. *Geophysical Journal International*, *79*(1), 235–255. https://doi.org/10.1111/j.1365-246X.1984.tb02853.x

Knopoff, L., Schwab, F., & Kauselt, E. (1973). Interpretation of Lg. *Geophysical Journal International*, *33*(4), 389–404. https://doi.org/10.1111/j.1365-246X.1973.tb02375.x

Krischer, L., Megies, T., Barsch, R., Beyreuther, M., Lecocq, T., Caudron, C., & Wassermann, J. (2015). ObsPy: A bridge for seismology into the scientific Python ecosystem. *Computational Science & Discovery*, *8*(1), 014003. https://doi.org/10.1088/1749-4699/8/1/014003

Lagardère, C., & Vargas, C. A. (2021). Earthquake distribution and lithospheric rheology beneath the Northwestern Andes, Colombia. *Geodesy and Geodynamics*, *12*(1), 1–10. https://doi.org/10.1016/j.geog.2020.12.002

Laske, G., Masters, G., Ma, Z., & Pasyanos, M. E. (2013). Update on CRUST1.0-A 1-degree global model of Earth's crust. *Geophysical Research Abstracts*(15), 2658. Retrieved from https://igppweb.ucsd.edu/~gabi/crust1.html

Leal-Mejía, H., Shaw, R. P., & Melgarejo I Draper, J. C. (2019). Spatial-temporal migration of granitoid magmatism and the Phanerozoic tectono-magmatic evolution of the Colombian Andes. In F. Cediel & R. P. Shaw (Eds.), *Geology and Tectonics of Northwestern South America* (pp. 253–410). Springer International Publishing. https://doi.org/10.1007/978-3-319-76132-9_5

Li, C., Van Der Hilst, R. D., Engdahl, E. R., & Burdick, S. (2008). A new global model for *P* wave speed variations in Earth's mantle. *Geochemistry, Geophysics, Geosystems*, *9*(5), Q05018. https://doi.org/10.1029/2007GC001806

Liu, Z., Zhao, L.-F., Xie, X.-B., Vargas, C. A., Tian, B.-F., & Yao, Z.-X. (2024). A new high-resolution broadband Lg attenuation model beneath Colombia: Implications for triple junction tectonics [Dataset]. *World Data Center for Geophysics*. https://doi.org/10.12197/2024GA008

Lonsdale, P. (2005). Creation of the Cocos and Nazca plates by fission of the Farallon plate. *Tectonophysics*, *404*(3–4), 237–264. https://doi.org/10.1016/j.tecto.2005.05.011

Lü, Y., Li, J., He, Y. H., Zhao, L. F., & Zhang, J. H. (2022). Velocity and anisotropic structure of the uppermost mantle beneath Central America and northwestern South America from Pn tomography. *Journal of Geophysical Research-Solid Earth*, *127*(4), e2021JB023643. https://doi.org/10.1029/2021JB023643

Luo, Y., Zhao, L.-F., Ge, Z.-X., Xie, X.-B., & Yao, Z.-X. (2021). Crustal Lg-wave attenuation in Southeast Asia and its implications for regional tectonic evolution. *Geophysical Journal International*, *226*(3), 1873–1884. https://doi.org/10.1093/gji/ggab122

Ma, X., Zhao, L.-F., Xie, X.-B., Chang, X., & Yao, Z.-X. (2023). Warm versus cold crust in the Tien Shan orogenic belt revealed by seismic Lg attenuation tomography. *Geophysical Journal International*, *233*(3), 2142–2154. https://doi.org/10.1093/gji/ggad055

McKenzie, D. P., & Morgan, W. J. (1969). Evolution of triple junctions. *Nature*, *224*(5215), 125–133. https://doi.org/10.1038/224125a0

Mendoza, V. (1977). Evolucion tectonica del Escudo de Guayana. In *II Congreso Latinoamericano de Geología, Caracas. ed. Memoria, Boletín de Geología, Caracas* (Vol. 7, pp. 2001–2270). Publ. Esp.

Miller, M. S., Levander, A., Niu, F., & Li, A. (2009). Upper mantle structure beneath the Caribbean-South American plate boundary from surface wave tomography. *Journal of Geophysical Research*, *114*(B1), 2007JB005507. https://doi.org/10.1029/2007JB005507

Mitchell, B. J., Pan, Y., Xie, J., & Cong, L. (1997). *Lg* coda *Q* variation across Eurasia and its relation to crustal evolution. *Journal of Geophysical Research*, *102*(B10), 22767–22779. https://doi.org/10.1029/97JB01894

Monsalve, G., Jaramillo, J. S., Cardona, A., Schulte-Pelkum, V., Posada, G., Valencia, V., & Poveda, E. (2019). Deep crustal faults, shear zones, and magmatism in the Eastern Cordillera of Colombia: Growth of a plateau from teleseismic receiver function and geochemical Mio-Pliocene volcanism constraints. *Journal of Geophysical Research: Solid Earth*, *124*(9), 9833–9851. https://doi.org/10.1029/2019jb017835

Montes, C., Rodriguez-Corcho, A. F., Bayona, G., Hoyos, N., Zapata, S., & Cardona, A. (2019). Continental margin response to multiple arc-continent collisions: The northern Andes-Caribbean margin. *Earth-Science Reviews*, *198*, 102903. https://doi.org/10.1016/j.earscirev.2019.102903

Mora-Páez, H., Kellogg, J. N., Freymueller, J. T., Mencin, D., Fernandes, R. M. S., Diederix, H., et al. (2019). Crustal defor mation in the northern Andes – A new GPS velocity field. *Journal of South American Earth Sciences*, *89*, 76–91. https://doi.org/10.1016/j.jsames.2018.11.002

Müller, R. D., Zahirovic, S., Williams, S. E., Cannon, J., Seton, M., Bower, D. J., et al. (2019). A global plate model including lithospheric deformation along major rifts and orogens since the Triassic. *Tectonics*, *38*(6), 1884–1907. https://doi.org/10.1029/2018TC005462

Ojeda, A., & Ottemöller, L. (2002). Q(Lg) tomography in Colombia. *Physics of the Earth and Planetary Interiors*, *130*(3–4), 253–270. https://doi.org/10.1016/S0031-9201(02)00010-9

Oliver, J., & Ewing, M. (1957). Higher modes of continental Rayleigh waves. *Bulletin of the Seismological Society of America*, *47*(3), 187–204. https://doi.org/10.1785/BSSA0470030187

Ottemöller, L. (2002). *Lg* wave *Q* tomography in Central America. *Geophysical Journal International*, *150*(1), 295–302. https://doi.org/10.1046/j.1365-246X.2002.01715.x

Paige, C. C., & Saunders, M. A. (1982). LSQR: An algorithm for sparse linear equations and sparse least squares. *ACM Transactions on Mathematical Software*, *8*(1), 43–71. https://doi.org/10.1145/355984.355989

Pardo, N., Cepeda, H., & Jaramillo, J. M. (2005). The Paipa volcano, Eastern Cordillera of Colombia, South America: Volcanic stratigraphy. *Earth Sciences Research Journal*, *9*(1), 3–18.

Pennington, W. D. (1981). Subduction of the eastern Panama Basin and seismotectonics of northwestern South America. *Journal of Geophysical Research*, *86*(B11), 10753–10770. https://doi.org/10.1029/JB086iB11p10753

Pérez-Forero, D., Koulakov, I., Vargas, C. A., Gerya, T., & Al Arifi, N. (2023). Lithospheric delamination as the driving mechanism of intermediate-depth seismicity in the Bucaramanga Nest, Colombia. *Scientific Reports*, *13*(1), 23084. https://doi.org/10.1038/s41598-023-50159-4

Phillips, W. S., & Stead, R. J. (2008). Attenuation of Lg in the western US using the USArray. *Geophysical Research Letters*, *35*(7), 2007GL032926. https://doi.org/10.1029/2007GL032926

Pindell, J., Kennan, L., Stanek, K. P., Maresch, W. V., & Draper, G. (2006). Foundations of Gulf of Mexico and Caribbean evolution: Eight controversies resolved. *Geológica Acta*, 303–341. https://doi.org/10.1344/105.000000371

Poveda, E., Julià, J., Schimmel, M., & Perez-Garcia, N. (2018). Upper and middle crustal velocity structure of the Colombian Andes from ambient noise tomography: Investigating subduction-related magmatism in the overriding plate. *Journal of Geophysical Research: Solid Earth*, *123*(2), 1459–1485. https://doi.org/10.1002/2017JB014688

Ramos, V. A., Cristallini, E. O., & Pérez, D. J. (2002). The Pampean flat-slab of the Central Andes. *Journal of South American Earth Sciences*, *15*(1), 59–78. https://doi.org/10.1016/S0895-9811(02)00006-8

Schenk, C. J., Viger, R. J., & Anderson, C. P. (1999). *Maps showing geology, oil and gas fields and geologic provinces of the South America region* (U.S. Geological Survey Open-File Report 97-470-D, p. 12). https://doi.org/10.3133/ofr97470D

Schmitz, M., Chalbaud, D., Castillo, J., & Izarra, C. (2002). The crustal structure of the Guayana Shield, Venezuela, from seismic refraction and gravity data. *Tectonophysics*, *345*(1–4), 103–118. https://doi.org/10.1016/S0040-1951(01)00208-6

Seton, M., Müller, R. D., Zahirovic, S., Gaina, C., Torsvik, T., Shephard, G., et al. (2012). Global continental and ocean basin reconstructions since 200Ma. *Earth-Science Reviews*, *113*(3–4), 212–270. https://doi.org/10.1016/j.earscirev.2012.03.002

Shen, L., Zhao, L.-F., Xie, X.-B., Yang, G., & Yao, Z.-X. (2023). Extremely weak Lg attenuation reveals ancient continental relicts in the South China block. *Earth and Planetary Science Letters*, *611*, 118144. https://doi.org/10.1016/j.epsl.2023.118144

Sun, M., Bezada, M. J., Cornthwaite, J., Prieto, G. A., Niu, F. L., & Levander, A. (2022). Overlapping slabs: Untangling subduction in NW South America through finite-frequency teleseismic tomography. *Earth and Planetary Science Letters*, *577*, 117253. https://doi.org/10.1016/j.epsl.2021.117253

Syracuse, E. M., Abers, G. A., Fischer, K., MacKenzie, L., Rychert, C., Protti, M., et al. (2008). Seismic tomography and earthquake locations in the Nicaraguan and Costa Rican upper mantle. *Geochemistry, Geophysics, Geosystems*, *9*(7). https://doi.org/10.1029/2008GC001963

Syracuse, E. M., Maceira, M., Prieto, G. A., Zhang, H. J., & Ammon, C. J. (2016). Multiple plates subducting beneath Colombia, as illuminated by seismicity and velocity from the joint inversion of seismic and gravity data. *Earth and Planetary Science Letters*, *444*, 139–149. https://doi.org/10.1016/j.epsl.2016.03.050

Syracuse, E. M., Van Keken, P. E., & Abers, G. A. (2010). The global range of subduction zone thermal models. *Physics of the Earth and Planetary Interiors*, *183*(1–2), 73–90. https://doi.org/10.1016/j.pepi.2010.02.004

Taboada, A., Rivera, L. A., Fuenzalida, A., Cisternas, A., Philip, H., Bijwaard, H., et al. (2000). Geodynamics of the northern Andes: Subductions and intracontinental deformation (Colombia). *Tectonics*, *19*(5), 787–813. https://doi.org/10.1029/2000TC900004

Van Benthem, S., Govers, R., Spakman, W., & Wortel, R. (2013). Tectonic evolution and mantle structure of the Caribbean. *Journal of Geophysical Research: Solid Earth*, *118*(6), 3019–3036. https://doi.org/10.1002/jgrb.50235

Vargas, C. A., Idarraga-Garcia, J., & Salazar, J. M. (2015). Curie point depths in northwestern South America and the southwestern Caribbean Sea. In C. Bartolini & P. Mann (Eds.), *Memoir 108: Petroleum Geology and Potential of the Colombian Caribbean Margin*. AAPG. https://doi.org/10.1306/13531936M1083642

Vargas, C. A., & Mann, P. (2013). Tearing and breaking off of subducted slabs as the result of collision of the Panama Arc-Indenter with northwestern South America. *Bulletin of the Seismological Society of America*, *103*(3), 2025–2046. https://doi.org/10.1785/0120120328

Vargas, C. A., Ochoa, L. H., & Caneva, A. (2019). Estimation of the thermal structure beneath the volcanic arc of the northern Andes by coda wave attenuation tomography. *Frontiers in Earth Science*, *7*, 208. https://doi.org/10.3389/feart.2019.00208

Veloza, G., Styron, R., & Taylor, M. (2012). *Open-source archive of active faults for northwest South America* (Vol. 22). GSA TODAY.

Wagner, L. S., Jaramillo, J. S., Ramírez-Hoyos, L. F., Monsalve, G., Cardona, A., & Becker, T. W. (2017). Transient slab flattening beneath Colombia. *Geophysical Research Letters*, *44*(13), 6616–6623. https://doi.org/10.1002/2017GL073981

Wang, Z., & Wei, D. (2018). Research progress on the formation and evolution of triple junctions of global plate motions. *Progress in Geophysics*, *33*(5), 1834–1843. https://doi.org/10.6038/pg2018BB0286

Weber, M., Duque, J. F., Hoyos, S., Cárdenas-Rozo, A. L., Gómez, J., & Wilson, R. (2020). The Combia volcanic province: Miocene post-collisional magmatism in the northern Andes. In *The Geology of Colombia* (Vol. 3, pp. 355–394). https://doi.org/10.32685/PUB.ESP.37.2019.12

Wessel, P., Luis, J. F., Uieda, L., Scharroo, R., Wobbe, F., Smith, W. H. F., & Tian, D. (2019). The generic mapping tools version 6. *Geochemistry, Geophysics, Geosystems*, *20*(11), 5556–5564. https://doi.org/10.1029/2019GC008515

Xie, X.-B., & Lay, T. (1994). The excitation of Lg waves by explosions: A finite-difference investigation. *Bulletin of the Seismological Society of America*, *84*(2), 324–342. https://doi.org/10.1785/BSSA0840020324

Yang, G., Chen, L., Zhao, L.-F., Xie, X.-B., & Yao, Z.-X. (2023). Crustal Lg attenuation beneath the Iranian Plateau: Implications for Cenozoic Magmatism related to slab subduction, slab break-off, and Mantle Flow. *Journal of Geophysical Research: Solid Earth*, *128*(3), e2022JB025664. https://doi.org/10.1029/2022JB025664

Yang, G., Zhao, L., Xie, X., He, X., Zhang, L., & Yao, Z. (2024). Strong Lg-wave attenuation reveals quarter-toroidal crustal melting around the Yakutat terrane in South-Central Alaska. *Journal of Geophysical Research: Solid Earth*, *129*(9), e2024JB029104. https://doi.org/10.1029/2024JB029104

Zhang, L., Zhao, L.-F., Xie, X.-B., Wu, Q.-J., & Yao, Z.-X. (2022). Lateral variations in crustal Lg attenuation in and around the Hangay Dome, Mongolia. *International Journal of Earth Sciences*, *111*(2), 591–606. https://doi.org/10.1007/s00531-021-02131-8

Zhao, L.-F., Xie, X.-B., He, J.-K., Tian, X., & Yao, Z.-X. (2013). Crustal flow pattern beneath the Tibetan Plateau constrained by regional Lg-wave Q tomography. *Earth and Planetary Science Letters*, *383*, 113–122. https://doi.org/10.1016/j.epsl.2013.09.038

Zhao, L.-F., Xie, X.-B., He, X., Shen, L., Zhang, L., & Yao, Z.-X. (2022). Seismic Lg-wave attenuation tomography: Method, algorithm, data processing flow and application. *Reviews of Geophysics and Planetary Physics*, *53*(6), 721–744. (in Chinese). https://doi.org/10.19975/j.dqyxx.2022-024

Zhao, L.-F., Xie, X.-B., Wang, W., Zhang, J., & Yao, Z.-X. (2010). Seismic Lg -wave Q tomography in and around Northeast China. *Journal of Geophysical Research*, *115*(B8), 2009JB007157. https://doi.org/10.1029/2009JB007157

Zhao, L.-F., Xie, X.-B., Wang, W.-M., Zhang, J.-H., & Yao, Z.-X. (2013). Crustal Lg attenuation within the North China Craton and its surrounding regions. *Geophysical Journal International*, *195*(1), 513–531. https://doi.org/10.1093/gji/ggt235

Zhu, H., Stern, R. J., & Yang, J. (2020). Seismic evidence for subduction-induced mantle flows underneath Middle America. *Nature Communications*, *11*(1), 2075. https://doi.org/10.1038/s41467-020-15492-6

Zhu, W., Zhao, L.-F., Xie, X.-B., He, X., Zhang, L., & Yao, Z.-X. (2023). High-resolution broadband Lg attenuation structure of the Anatolian crust and its implications for mantle upwelling and Plateau uplift. *Geophysical Research Letters*, *50*(6), e2023GL103470. https://doi.org/10.1029/2023GL103470

References From the Supporting Information

Castro, R. R., Anderson, J. G., & Singh, S. K. (1990). Site response, attenuation and source spectra of S-waves along the Guerrero, Mexico, subduction zone. *Bulletin of the Seismological Society of America*, (80), 1481–1503.

He, X., Zhao, L.-F., Xie, X.-B., Zhang, L., & Yao, Z.-X. (2023). Eastward expansion of the Tibetan plateau: Insights from stress drops of the 2021 Ms 6.4 Yangbi, Yunnan and Ms 7.4 Maduo, Qinghai earthquake sequences in China. *Frontiers in Earth Science*, *11*, 1081605. https://doi.org/10.3389/feart.2023.1081605

Herrmann, R. B., & Kijko, A. (1983). Short-period *Lg* magnitudes: Instrument, attenuation, and source effects. *Bulletin of the Seismological Society of America*, *73*(6A), 1835–1850. https://doi.org/10.1785/BSSA07306A1835

Schlittenhardt, J. (2001). Teleseismic Lg of Semipalatinsk and Novaya Zemlya nuclear explosions recorded by the GRF (Gräfenberg) array: Comparison with regional Lg (BRV) and their potential for accurate yield estimation. *Pure and Applied Geophysics*, *158*(11), 2253–2274. https://doi.org/10.1007/PL00001148

Street, R. L., Herrmann, R. B., & Nuttli, O. W. (1975). Spectral characteristics of the Lg wave generated by Central United States earthquakes. *Geophysical Journal International*, *41*(1), 51–63. https://doi.org/10.1111/j.1365-246X.1975.tb05484.x

Zhao, L.-F., & Mousavi, S. M. (2018). Lateral variation of crustal Lg attenuation in eastern North America. *Scientific Reports*, *8*(1), 7285. https://doi.org/10.1038/s41598-018-25649-5